

## 197. A New Helicopodand: Molecular Recognition of Dicarboxylic Acids with High Diastereoselectivity

by Linda Owens<sup>a</sup>), Carlo Thilgen<sup>a</sup>), François Diederich<sup>a</sup>)\*, and Carolyn B. Knobler<sup>b</sup>)

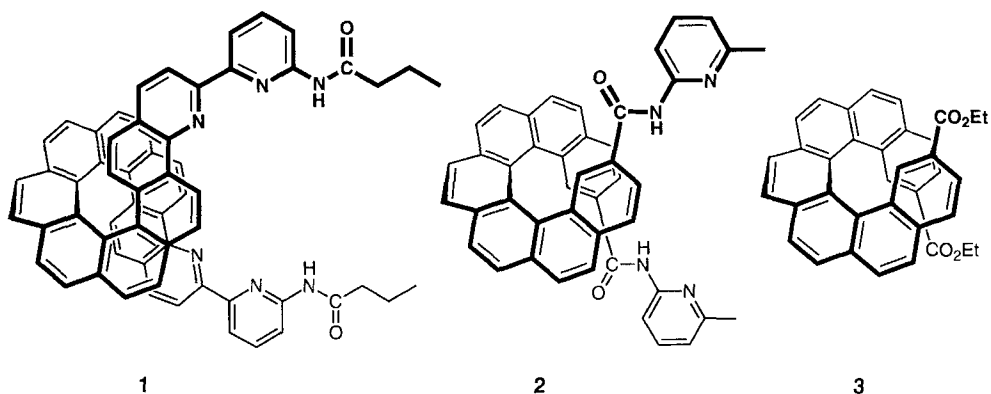
<sup>a</sup>) Laboratorium für Organische Chemie der Eidgenössischen Technischen Hochschule, ETH-Zentrum,  
Universitätstrasse 16, CH-8092 Zürich

<sup>b</sup>) Department of Chemistry and Biochemistry, University of California, Los Angeles, California 90024-1569

(10. IX. 93)

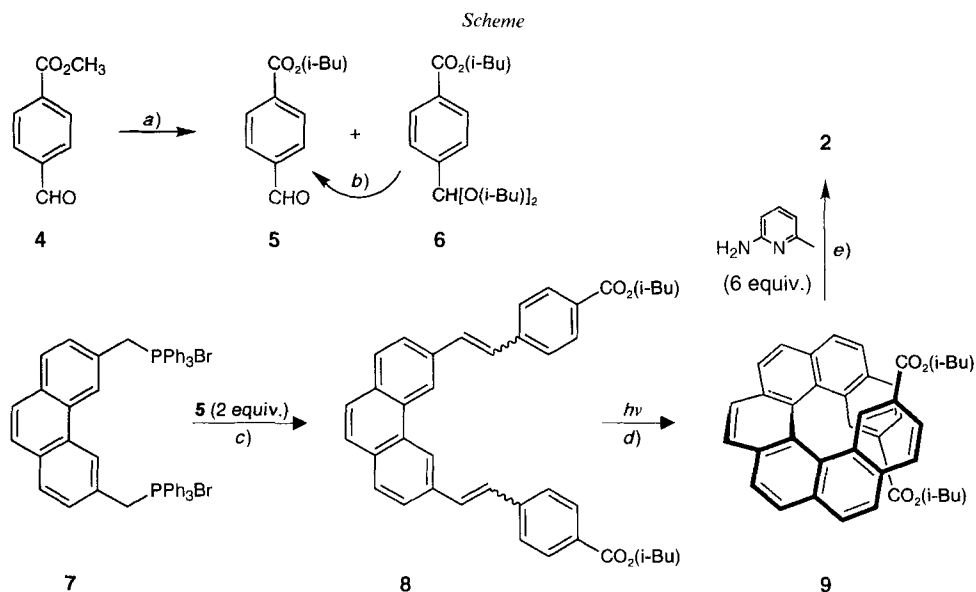
The helicopodand (*PM*)-**2** is prepared following the photocyclodehydrogenation route to helicenes (*Scheme*). At the ends of a [7]helicene backbone, this acyclic receptor ('podand') possesses a H-bonding recognition site shaped by two convergent *N*-(pyridin-2-yl)carboxamide (CONH(py)) units. In the crystal of diethyl [7]helicene-2,17-dicarboxylate ((*PM*)-**3**), a direct synthetic precursor of **2**, molecules of the same chirality form stacks, and two stacks of opposite chirality are interlocked in a pair having average face-to-face aromatic contacts of 3.82 Å between benzene rings of different enantiomers (*Fig. 2*). In contrast, two conformations are observed in the crystal structure of **2**, one with both CONH(py) residues pointing with their H-bonding centers NH/N away from the binding site ('out-out') and a second ('in-out') with one of the two CONH(py) residues pointing towards the binding site ('in'; *Fig. 4*). While no H-bonding network propagates throughout the crystal, enantiomers of **2** in the different conformations 'out-out' and 'in-out' form H-bonded pairs that are further stabilized by a H-bond to one molecule of CHCl<sub>3</sub>. In the productive 'in-in' conformation, **2** forms stable 1:1 complexes with  $\alpha,\omega$ -dicarboxylic acids in CHCl<sub>3</sub>, and a diastereoselectivity in complexation of  $\Delta(\Delta G^\circ) = 1.4 \text{ kcal mol}^{-1}$  is measured for two substrates differing only in the (*E*)/(*Z*)-configuration at their double bond (see *Table 2*). A comprehensive force-field molecular-modeling study suggests that only the (*E*)-derivative possesses the correct geometry for a ditopic four-fold H-bonding interaction between its two COOH residues and the two CONH(py) groups in **2** (*Fig. 5*). With *N,N'*-bis[(benzyloxy)carbonyl]-L-cystine, the formation of diastereoisomeric complexes with (*PM*)-**2** is observed (*Fig. 7*).

**1. Introduction.** – Using small synthetic molecules to mimic nature's ability to distinguish between the enantiomers of chiral substances has long been a goal of chemists. Early studies in chiral molecular recognition showed the effectiveness of optically active crown ethers incorporating binaphthyl [1] and spirobifluorenyl [2] spacers in complexing amino-acid esters and chiral primary ammonium ions with high enantioselectivity. More recently, a variety of optically active clefts [3–6] and cyclophanes [7] were introduced to selectively recognize enantiomers of neutral chiral substrates through multiple H-bonding interactions [8]. Studies with these systems showed that high conformational homogeneity of a chiral receptor favors high enantioselectivity since it prevents geometric adjustments leading to a favorable accommodation of both substrate enantiomers in the binding site [4b] [7]. Among the more rigid known chiral shapes are helicenes [9] [10], and this led us to introduce a helicene as a chiral backbone into the helicopodand **1** [11], an acyclic receptor ('podand') [12] with a chiral cleft binding site lined with convergent H-bonding functionality provided by two *N*-(pyridin-2-yl) amide (CONH(py)) residues [13] [14]. Unfortunately, two high-dilution photocyclodehydrogenations [15] in the synthesis of dipyrido[9]helicene derivative **1** prevented its preparation in sufficient quantities for meaningful molecular-recognition studies and, therefore, the potential receptor quali-



ties of **1** could not be explored. In a new test of the helicopodand concept [11] [16], the synthetically more readily accessible helicopodand **2** which incorporates a [7]helicene backbone, was prepared by a synthetic sequence which includes only one high-dilution photocyclodehydrogenation. Here, we report the synthesis, X-ray crystallographic structural determination, and molecular-recognition properties of racemic (*PM*)-**2**. Also, in view of the recent interest in H-bonded helical supramolecular arrays in solid-state structures [17], the crystal packing of **2** and diester **3** are analyzed in more detail [18].

**2. Results and Discussion.** – 2.1. *Synthesis.* Following established protocols for [7]helicene formation [15], the synthesis of **2** was accomplished in good yield starting from



*a*) *i*-BuOH, TsOH, 180°. *b*) 0.12N HCl, 1,4-dioxane, 20°, 58% (steps *a* and *b*). *c*) Na(*i*-BuO), *i*-BuOH, THF, r.t., 80%. *d*) I<sub>2</sub>, methyloxirane, *hν* (high-pressure Hg), toluene, r.t., 52%. *e*) BuLi (6 equiv.), THF, r.t., 93%.

**5** (obtained from **4** and **6**) and **7** via **8** and the bis(isobutyl ester) **9** (*Scheme*). In the photocyclodehydrogenation of **8** to **9** under  $N_2$  in the presence of  $I_2$  as oxidizing agent, methyloxirane was added to scavenge the HI which forms during the reaction [10a]. Initially, the bis(ethyl ester) **3** was prepared *via* a similar route as precursor of **2**; however, the ethyl analogue of stilbene **8** proved to be too insoluble in toluene for convenient use in the photocyclization reaction. Nevertheless, sufficient quantities of **3** were produced to grow X-ray-quality crystals. The final amide-bond formations to **2** were conveniently achieved in good yield by direct reaction of diester **9** with the anion of 6-methylpyridin-2-amine.

**2.2. X-Ray Crystal Structures of (PM)-2 and (PM)-3.** Diester **3** (*Fig. 1*) crystallized from  $CHCl_3$  in the  $P\bar{1}$  space group with 2 molecules per unit cell. The structure was determined at  $25^\circ$ , and the final discrepancy factor  $R$  was 0.079. Bond lengths, bond and torsional angles, and intramolecular distances in **3** closely resemble those previously found in the crystal structures of [7]helicenes [18d–f]. Significant C,C-bond alternation is observed in the helix, the C(28)–C(29) bond being the shortest with 1.343(6) Å and the C(19)–C(23) bond the longest with 1.459(5) Å [18]. The torsional angles at the inner helical rim are all different and vary between  $18.6(5)^\circ$  for C(11)–C(10)–C(15)–C(19) and  $25.4(5)^\circ$  for C(15)–C(19)–C(23)–C(27) (*Table 1*). The overlapping terminal rings in the [7]helicene are separated by greater than *Van der Waals* distance on the outside of the helix (C(8)–C(33) = 4.45 Å; C(7)–C(32) = 4.90 Å) but come into very close contact on the interior of the helix (C(11)–C(31) = 3.14 Å; C(10)–C(35) = 3.12 Å, *Table 1*).

In the crystal, molecules of **3** of the same chirality form stacks, and two stacks of opposite chirality are interlocked in a pair which brings benzene rings of (*P*)- and (*M*)-enantiomers into a face-to-face type orientation with an average distance of 3.82 Å

Table 1. Selected Intramolecular Distances and Torsional Angles Observed in the X-Ray Crystal Structures of **2** and **3**<sup>a)</sup>

	(PM)-2		(PM)-3	
	'out-out'	'in-out'		
Distance [Å]			Distance [Å]	
C(13)–C(38)	4.72	4.36	C(8)–C(33)	4.45
C(12)–C(37)	4.64	4.37	C(7)–C(32)	4.90
C(16)–C(36)	3.14	3.19	C(11)–C(31)	3.14
C(15)–C(40)	3.15	3.16	C(10)–C(35)	3.12
C(11)–C(39)	5.23	5.33	C(6)–C(34)	5.20
C(9)–C(41)	7.54	7.95	C(4)–C(36)	7.64
N(8)–N(42)	8.24	9.06	O(3)–O(38)	8.45
Torsional angle [°] <sup>b)</sup>			Torsional angle [°] <sup>b)</sup>	
C(28)–C(32)–C(36)–C(40)	14.5	25.5	C(23)–C(27)–C(31)–C(35)	20.0
C(21)–C(28)–C(32)–C(36)	22.8	22.7	C(19)–C(23)–C(27)–C(31)	21.9
C(20)–C(21)–C(28)–C(32)	29.0	26.6	C(15)–C(19)–C(23)–C(27)	25.4
C(15)–C(20)–C(21)–C(28)	19.9	20.9	C(10)–C(15)–C(19)–C(23)	25.0
C(16)–C(15)–C(20)–C(21)	18.3	24.6	C(11)–C(10)–C(15)–C(19)	18.6

<sup>a)</sup> Although the crystallographic numberings of **2** and **3** are different (see *Figs. 1* and *3*), data in each line are given for corresponding intramolecular atom distances and torsional angles, respectively, and can be directly compared.

<sup>b)</sup> Standard deviation:  $0.5^\circ$ .

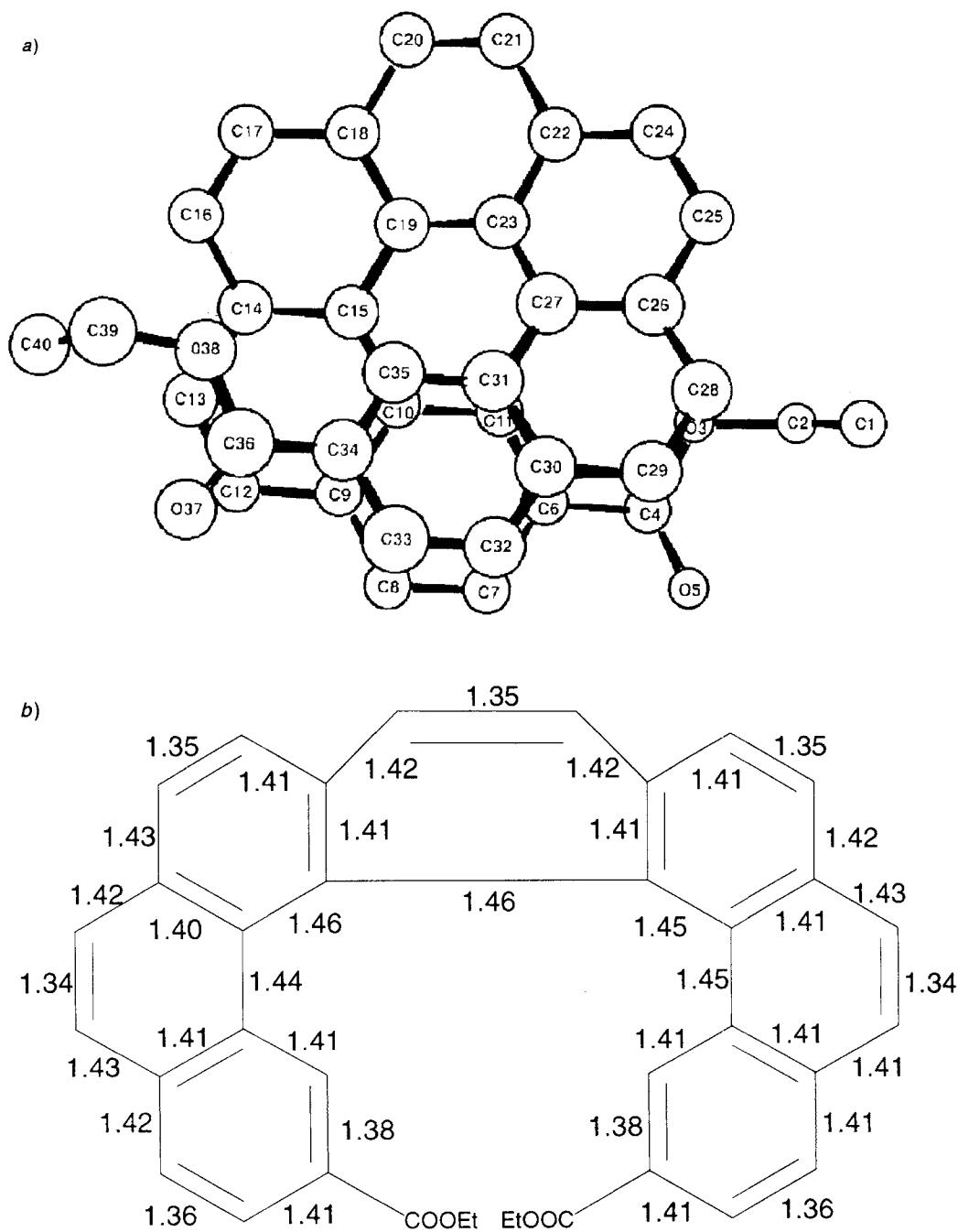


Fig. 1. Molecular structure of diester (PM)-3 a) in a view down the helix axis and b) bond lengths in the [7]helicene backbone. Arbitrary numbering.

between aromatic rings (Fig. 2). Comparatively weaker interactions exist between the pairs of helicene stacks.

Helicopodand (PM)-2 crystallized from  $\text{CHCl}_3$  in the  $P2_1/a$  space group with 8 molecules per unit cell, and its structure was determined at  $25^\circ$  with a final discrepancy factor  $R$  of 0.123. For each enantiomer of 2, two conformers with respect to the rotation around the  $\text{C}(\text{Ar})\text{--}\text{C}(\text{O})$  bond were found in the crystal structure: one with the H-bond-

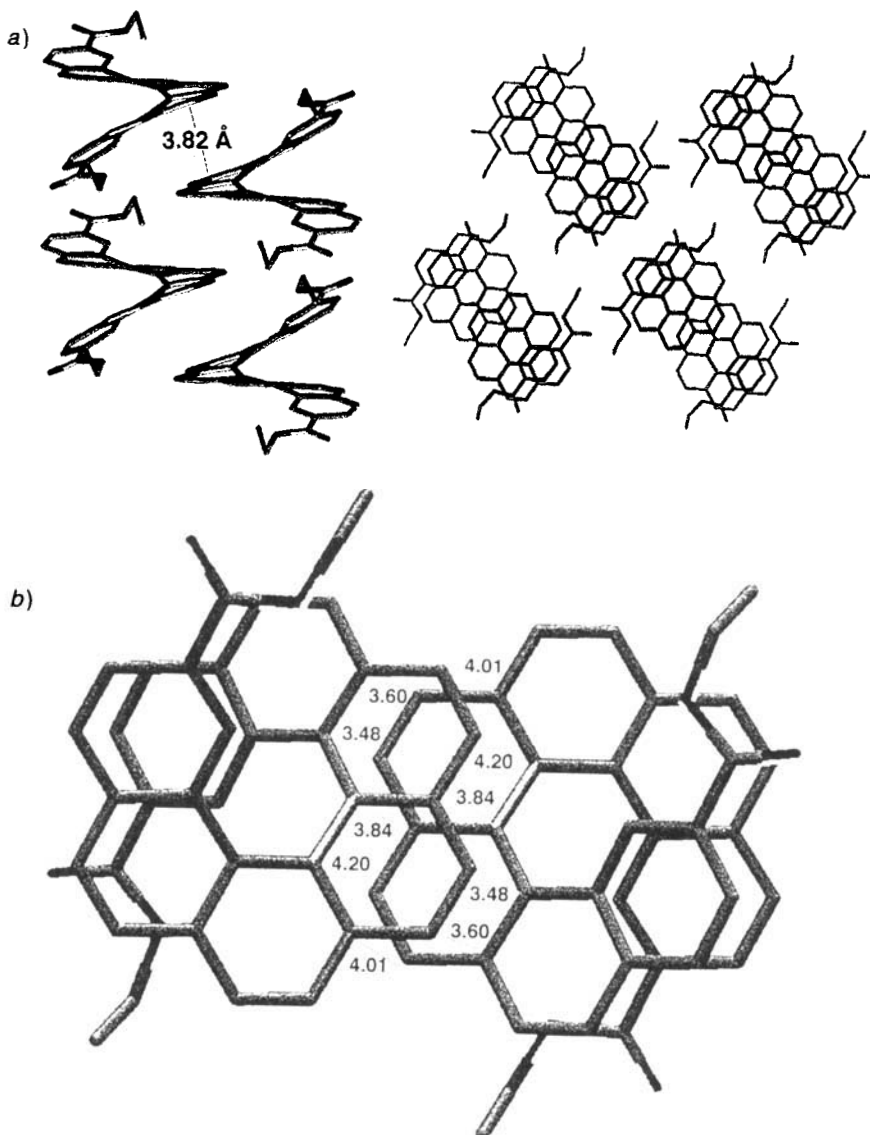


Fig. 2. Crystal packing of (PM)-3 showing a) a pair of interlocking stacks of enantiomers (left) and the orientation between pairs in the crystal (right) and b) the face-to-face aromatic interactions in a pair of interlocking stacks

ing functionality NH/N of the two CONH(py) groups pointing out of the binding site ('out-out') and a second one with the H-bonding groups pointing inside and outside the binding site ('in-out'), respectively. A space-filling model and a labeled view of the 'in-out' conformation perpendicular to the helix axis are shown in Fig. 3. Bond lengths and angles in both conformers of **2** closely resemble those found in **3**. However, large differences exist between comparable intramolecular distances and torsional angles in the three helices (Table 1). These differences, particularly between the two conformers of (PM)-**2**, provide yet another nice example for the significant flexibility of fused aromatic ring structures [18] [19].

While no continuous H-bonding network propagates throughout the crystal, enantiomers of host **2** do form H-bonded pairs which are further stabilized by the interaction

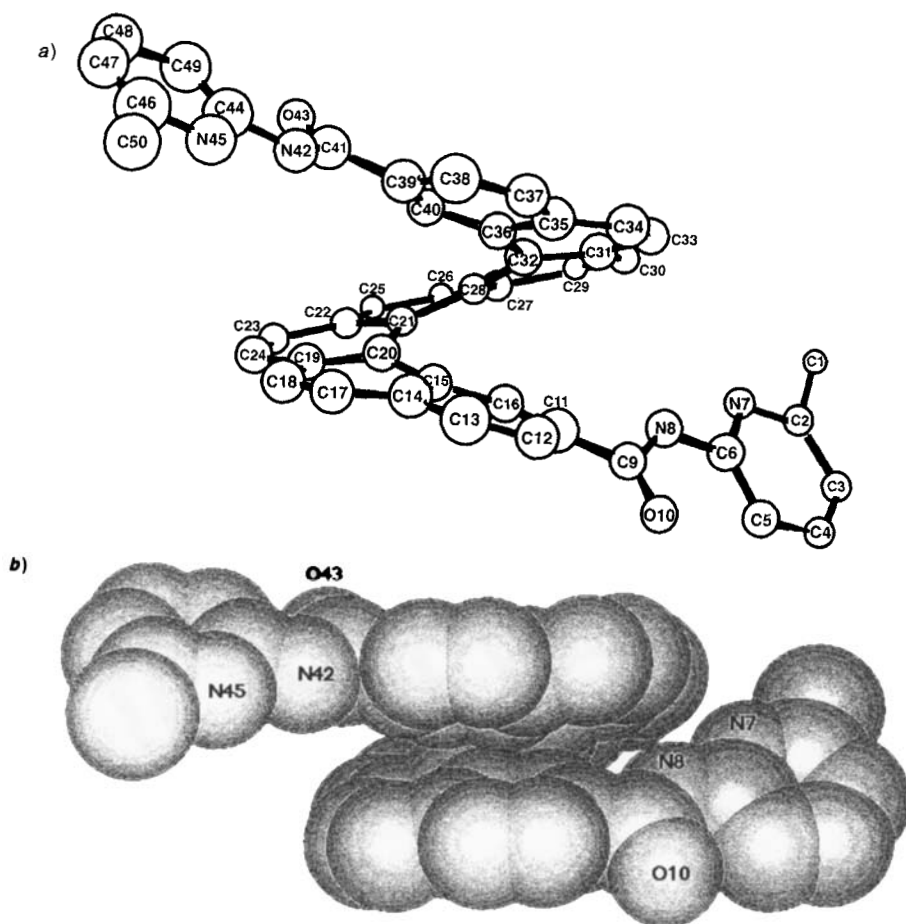


Fig. 3. Molecular structure of the 'in-out'-conformer of helicopodand (PM)-**2** a) in a view perpendicular to the helix axis and b) in a space-filling representation. Arbitrary numbering.

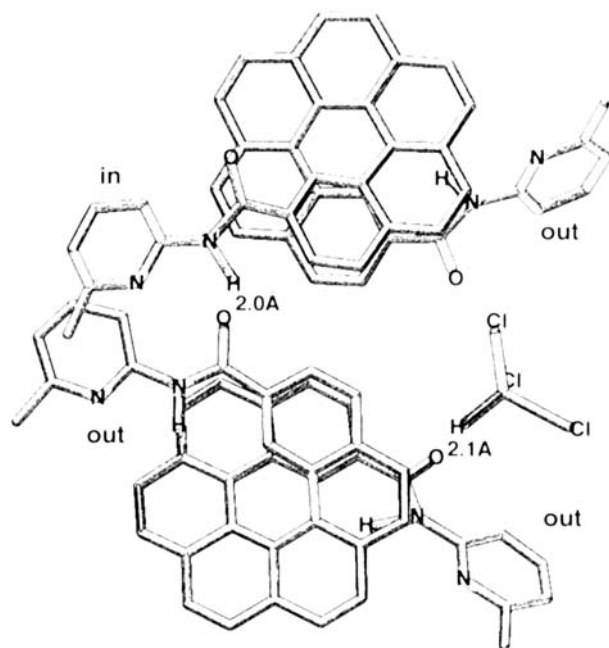


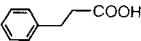
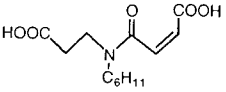
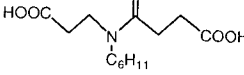
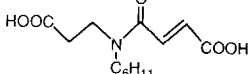

Fig. 4. Crystal packing of (PM)-2 showing a H-bonded pair of two enantiomers with different conformations ('in-out' and 'out-out') and the H-bonding of the pair to one molecule of CHCl<sub>3</sub>

with one molecule of CHCl<sub>3</sub>, the solvent used for recrystallization (Fig. 4). Interestingly, the enantiomers in such a pair do not possess identical geometries but, rather, one enantiomer adopts the 'in-out' and the other the 'out-out' conformation.

Force-field-computational studies were previously proven quite effective for modeling helicenes [11] [20]. Molecular-mechanics calculations [21–24] using the MM3\* force field [22] as implemented in MacroModel v.3.5. [25] (see *Exper. Part* for details) predicted that for isolated molecules of **2** in CHCl<sub>3</sub> solution, the 'out-out' form should be *ca.* 2 kcal/mol more stable than the 'in-out' form. Obviously, for the planned ditopic complexation of  $\alpha,\omega$ -dicarboxylic acids, the more stable unproductive 'out-out' and 'in-out' conformations of **2** will first have to change into the productive 'in-in' conformation in which the H-bonding functionalities NH/N of the two CONH(py) moieties converge into the binding site. This reorganization will occur at the expense of parts of the intrinsic binding free energy.

**2.3. Complexation Studies with Helicopodand 2 and  $\alpha,\omega$ -Dicarboxylic Acids.** The initial selection of suitable dicarboxylic-acid guests for (PM)-**2** was done with the help of CPK molecular models. Subsequently, quantitative complexation studies using <sup>1</sup>H-NMR titrations were performed in dry CDCl<sub>3</sub> at 300 K using a constant concentration of host ([**2**]  $\approx$  1 mM) and variable guest concentrations in the range of 0.3 to 6.0 mM (see Table 5, in *Exper. Part*). The complexation-induced changes in chemical shift of selected protons of **2** were evaluated by a non-linear least-squares analysis to calculate association con-

Table 2. Stabilities of 1:1 Complexes Formed between Helicodand **2** and  $\alpha,\omega$ -Dicarboxylic Acids in  $\text{CDCl}_3$  Determined at 300 K by  $^1\text{H-NMR}$  Titrations

Guest	$K_a$ [ $1 \text{ mol}^{-1}$ ]	$-\Delta G^0$ [kcal/mol]
 <b>10</b>	$280 \pm 60$	$3.29 \pm 0.13$
 <b>11</b>	$230 \pm 40$	$3.24 \pm 0.15$
 <b>12</b>	$1390 \pm 140$	$4.31 \pm 0.10$
 <b>13</b>	$2610 \pm 410$	$4.68 \pm 0.16$
 <b>14</b>	$5500 \pm 810$	$5.04 \pm 0.10$

$\text{C}_6\text{H}_{11}$  = cyclohexyl

stants  $K_a$  and binding free energies  $-\Delta G^0$  (Table 2). The cyclohexyl groups in **11**–**13** were attached to provide suitable solubility of these substrates in  $\text{CDCl}_3$ .

The strength of monotopic binding between one COOH residue and one CONH(py) group was determined in the titration with 3-phenylpropanoic acid (**10**). In all cases but one, the dicarboxylic acids exhibited much stronger binding than **10** (Table 2), and we take this as strong evidence that both COOH functions participate in the host-guest association (ditopic binding) [13] [14] (for dicarboxylic-acid binding, see [26]). Heptanedioic acid (**14**) forms the most stable complex. MM3\* force-field calculations showed that the amide protons NH of **2** in the productive 'in-in'-conformation are separated by 7.98 Å. In fully staggered **14**, the C=O groups are separated by 7.77 Å. The high binding constant can, therefore, be explained by a good match of the lowest-energy conformation of the guest with the conformation required to bind in a ditopic way to 'in-in'-**2**. In a fully staggered geometry, the two C(OH)=O groups of **12** (9.81 Å) and **13** (9.36 Å) are too far apart for a good association with the two NH groups of 'in-in'-**2**, and these guests adopt binding geometries with one *gauche* conformation (see Fig. 5 below). This could explain their weaker binding compared to **14**. Diacid **13** binds better than **12**, since the (*E*)-double bond enhances its preorganization.

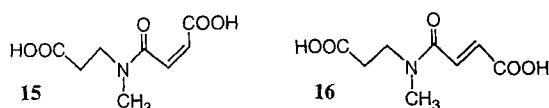
While the (*E*)-diacid **13** was one of the strongest binders ( $-\Delta G^0 = 4.68 \text{ kcal mol}^{-1}$ ), the corresponding (*Z*)-diacid **11** only showed an association strength ( $-\Delta G^0 = 3.24 \text{ kcal mol}^{-1}$ ) similar to the value measured for phenylpropanoic acid **11** ( $-\Delta G^0 = 3.29 \text{ kcal mol}^{-1}$ ). The close similarity in the binding strength between **10** and **11** initially suggested that the high diastereoselectivity of **2** for the diastereoisomeric guests **11** and **13** ( $\Delta(\Delta G^0) = 1.4 \text{ kcal mol}^{-1}$ ) was due to weak, monotopic binding of **11**, involving only one of its two COOH residues. However, MM3\* calculations showed that, in a staggered conformation, the two C(OH)=O groups in **11** are separated by 8.59 Å, a sufficient



spacing to reach to the two amide NH protons of 'in-in'-**2**. Furthermore, the analysis of the complexation-induced changes in  $^1\text{H}$ -NMR chemical shift calculated for saturation binding ( $\Delta\delta(\text{sat})$ ; see *Table 5* in *Exper. Part*) provided clear evidence, that both NH protons of **2** participate in the binding of **11**.

Complexation-induced downfield shifts of *ca.* 2 ppm are generally observed for the resonances of NH protons H-bonded to carbonyl O-atoms in  $\text{CDCl}_3$  [13] [14]. A shift of only half that size ( $\Delta\delta(\text{sat})$  0.93 ppm) was found for the NH resonance of **2** in the monotopic 1:1 complex with 3-phenylpropanoic acid (**10**) since, at fast host-guest exchange, this signal appears at the average of the chemical shifts of one bound and one free NH. If the (*Z*)-diacid **11** would also undergo monotopic binding to one CONH(py) only, the magnitude of the complexation-induced shift of the NH resonance of **2** would be similar to that observed in the complex **2**·**10**. However, the shift of this resonance in the complex **2**·**11** was  $\Delta\delta(\text{sat})$  2.05 ppm, which is the value expected for the full participation of both NH protons in the H-bonding to the guest and corresponds to the shifts observed in the complexes **2**·**12** and **2**·**13**. To explore the binding geometries of the diastereoisomeric acids **11** and **13** and to find the origin of the high diastereoselectivity, a comprehensive molecular-modeling study was undertaken. For computational-time reasons, diacids **15** and **16**, in which the cyclohexyl groups of **11** and **13** are replaced by Me groups, were used in this study.

In the modeling study, 1000 step Monte Carlo (MC) simulations in BatchMin [27] using the united atom AMBER\* force field [23] and the GB/SA solvation model [28] for  $\text{CHCl}_3$  were first carried out on free **15** and **16** to see if either compound were forming intramolecular H-bonds. For compound **15**, 40 structures and for **16**, 20 structures were found within 50 kJ mol $^{-1}$  of the global minimum. None of these structures was intramolecularly H-bonded. Neither **15** nor **16** possess intramolecular H-bonds that must be disrupted to achieve a binding conformation. The diastereoselectivity of **2** must, therefore, originate from differences in host-guest complementarity.



Complexes **2**·**15** and **2**·**16** were submitted for 2000 step MC searches using GB/SA  $\text{CHCl}_3$  solvation and both the MM3\* and AMBER\* force fields in MacroModel v.3.5. The output structures of the AMBER\* search were also further minimized within the OPLS\* force field [24]. All three force fields found the ditopic binding mode of **16** with the participation of both COOH groups of the guest. In AMBER\* and OPLS\*, global minima were found for the complex **2**·**16** with four H-bonds between the two COOH and CONH(py) NH/N-groups, corresponding to the maximal possible H-bonding interaction (*Fig. 5*). In the lowest-energy MM3\* structure, one COOH group binds to the NH/N functions of one 'in'-CONH(py) moiety, whereas the second COOH group forms a  $\text{O}-\text{H}\cdots\text{O}=\text{C}$  H-bond to the amide C=O of the second CONH(py) group, which adopts the 'out'-conformation. The simulations with all three force fields generated several additional conformers with full ditopic binding (4 H-bonds) within 2 kcal/mol of the calculated global minima (*Table 3*, *Fig. 6*). The only significant alternative binding mode

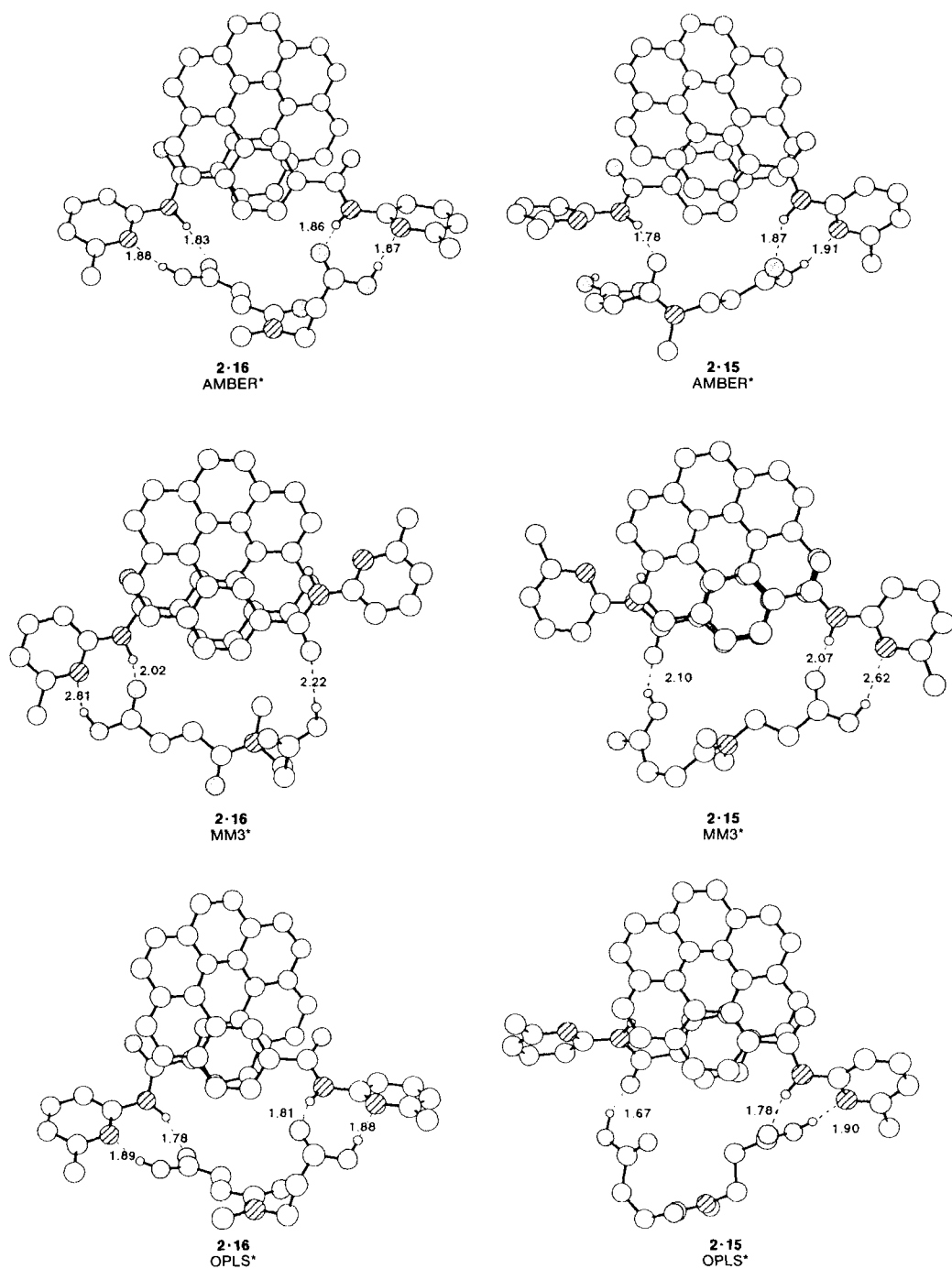


Fig. 5. Lowest-energy conformations of complexes **2·16** and **2·15** as computed by AMBER\*, MM3\*, and OPLS\*

found in the calculations is the one observed in the lowest-energy MM3\* structure. However, this binding mode is not in agreement with the experimental NMR data, which require participation of both NH groups of the helicopodand in guest binding.

Table 3. Conformers of Complexes **2·15** and **2·16** within 2 kcal/mol of the Global Minima Generated by the AMBER\*, MM3\*, and OPLS\* Force Fields<sup>a)</sup>

Force field	Complex <b>2·16</b>				Complex <b>2·15</b>			
	$\Delta E$ [kcal/mol]	H-Bonds	Host-guest H-bonds to the two CONH(py) groups		$\Delta E$ [kcal/mol]	H-Bonds	Host-guest H-bonds to the two CONH(py) groups	
			(1)	(2)			(1)	(2)
AMBER*	0	4	a, b	a, b	0	3	a, b	c
	0.63	3	a, b	d	0.95	3	a, b	d
	0.67	4	a, b	a, b	1.17	3	a, b	b
	1.49	4	a, b	a, b	1.22	3	a, b	c
	1.75	4	a, b	a, b	1.32	4	a, b	a, b
	1.76	3	a, b	d	1.52	4	a, b	a, b
					1.52	4	a, b	a, b
					1.63	3	a, b	c
					1.76	4	a, b	a, b
					1.95	3	a, b	d
MM3*	0	3	a, b	d	0	3	a, b	d
	0.35	1	d		1.84	3	a, b	c
	0.69	2	a	d	2.01	3	a, b	c
	0.94	3	a, b	a				
	0.98	4	a, b	a, b				
	1.15	4	a, b	a, b				
	1.49	4	a, b	a, b				
	1.49	3	a, b	d				
	1.76	3	a, b	d				
	1.94	1	d					
	1.99	1	a					
OPLS*	0	4	a, b	a, b	0	3	a, b	d
	0.88	3	a, b	d	0.47	4	a, b	a, b
	0.91	4	a, b	a, b	1.00	3	a, b	c
	1.53	3	a, b	d	1.38	3	a, b	c
					1.46	2	b	c
					1.71	4	a, b	a, b
					1.92	4	a, b	a, b

<sup>a)</sup> The H-bond labels a, b, c, and d are shown in Fig. 6.

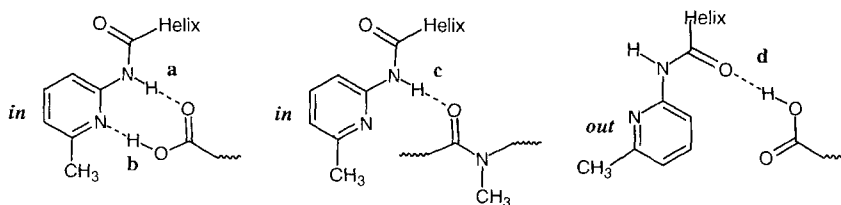


Fig. 6. Host-guest H-bonds found in the simulations for **2·15** and **2·16**

The weaker H-bonding association between **15** and **2** was also reproduced in the modeling study, although more divergent results were obtained. The simulations with all three force fields clearly showed that, in contrast to the complex **2**·**16**, the two H-bonds between the COOH and the basic pyridine N-atoms, which are crucial for high association strength [4b] [14b], cannot be well established in the complex **2**·**15**. Apparently, there exists no good binding conformation of **15** in which both acidic OH groups reach to the two pyridine N-atoms.

The lowest-energy structure generated with AMBER\* nicely reproduced the <sup>1</sup>H-NMR data by showing the participation of both NH functions of **2** in the H-bonding to the guest. One COOH group of **15** forms H-bonds to the N/NH functions of one CONH(py), and the amide C=O of the guest forms a H-bond to the second NH of **2** (Fig. 5). The participation of both NH groups accounts for the  $\Delta\delta(\text{sat})$  of 2.05 ppm, and the failure of one COOH to reach the pyridine N-atom accounts for the less favorable binding energy. OPLS\* found one COOH group doubly H-bonded to one 'in'-CONH(py) and the other

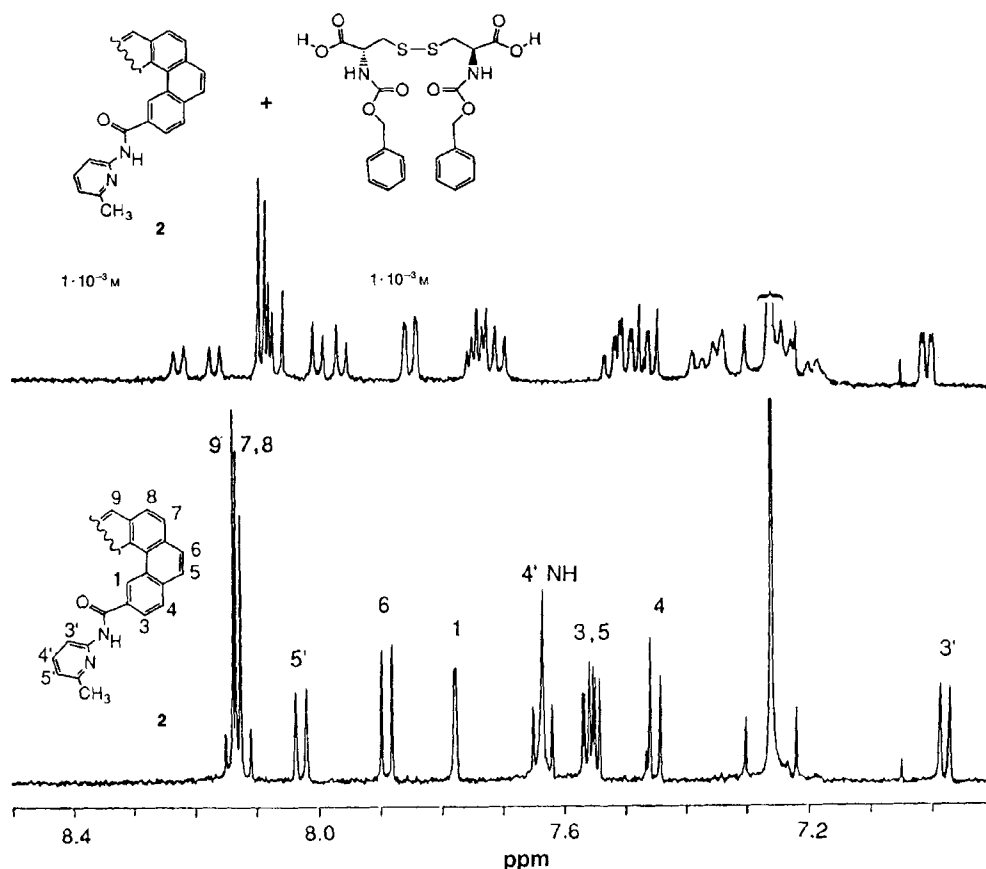


Fig. 7. <sup>1</sup>H-NMR spectrum (CDCl<sub>3</sub>, 300 K) of a 1:1 mixture of **2** and N,N'-bis[(benzyloxy)carbonyl]-L-cystine ( $c = 1 \text{ mM}$ ). The numbering of the helicopodand is arbitrary.

OH residue bound to the C=O group of the second CONH(py) which adopts the 'out'-conformation. A similar bonding pattern is seen in the MM3\* structure of **2**·**15**. The conformational sampling within 2 kcal/mol of the calculated global minima yielded in all three force fields a significant number of structures with the H-bonding pattern seen in the lowest-energy AMBER\* geometry, which reproduce the NMR data (Table 3).

From the modeling studies, we conclude that the diastereoselectivity observed between **11** and **13** arises from the failure of **11** to reach the pyridine N-atoms of **2** with both OH groups forming the two energetically most relevant H-bonds, and not from breakage of H-bonds within the uncomplexed guest molecules.

The ability of **2** to form diastereoisomeric complexes of different geometry and, possibly of different energy, was tested in a study with a chiral disulfide. A screening of commercially available  $\alpha,\omega$ -dicarboxylic acids had shown that **2** formed complexes with dithiobis(nicotinic acid) and 3,3'-dithiobis(propanoic acid). When the <sup>1</sup>H-NMR spectrum of an equimolar (1 mM) solution of optically active *N,N'*-bis[(benzyloxy)carbonyl]-L-cystine and **2** was compared to the spectrum of pure **2**, large differential complexation-induced shifts in the proton resonances of **2** were observed, and doubling of each resonance indicated the formation of diastereoisomeric complexes (Fig. 7). A determination of differential stabilities of these complexes awaits the optical resolution of **2**.

**3. Conclusion.** – The X-ray structural analysis showed very different crystal packing motifs for the [7]helicene derivatives (*PM*)-**2** and (*PM*)-**3**. In the crystal of **3**, molecules of the same chirality form stacks, and two stacks of opposite chirality are interlocked in a pair having average face-to-face aromatic contacts of 3.82 Å between benzene rings of different enantiomers, whereas enantiomers of **2** associate *via* H-bonding to dimers that are further stabilized by interaction with one molecule of included solvent (CHCl<sub>3</sub>). Interestingly, enantiomers of **2** in such a dimer adopt different conformations with respect to the orientation of the two CONH(py) groups. Torsional angles and intramolecular distances in the [7]helicene backbones in **3** and the two conformers of **2** differ significantly from each other providing another example for the considerable flexibility of fused benzene ring structures. With **2**, we could for the first time show the validity of our helicopodand concept for receptor design [11]. In the productive 'in-in' conformation with the two CONH(py) groups converging with their NH/N functionality into the binding site, **2** forms stable 1:1 complexes with  $\alpha,\omega$ -dicarboxylic acids in CHCl<sub>3</sub>, and a diastereoselectivity in complexation of  $\Delta(\Delta G^0) = 1.4$  kcal mol<sup>-1</sup> was measured for the substrates **11** and **13** which differ only by the (*Z*)/(*E*)-configuration at their double bond. A comprehensive force-field molecular-modeling study suggested that only the (*E*)-derivative possesses the correct geometry for a four-fold ditopic H-bonding interaction between its two COOH residues and the two CONH(py) groups of **2**. A preliminary study with *N,N'*-bis[(benzyloxy)carbonyl]-L-cystine showed that the racemic helicopodand (*PM*)-**2** forms diastereoisomeric complexes of different geometry. Whether these complexes differ also in their stability remains to be determined following the resolution of (*PM*)-**2**. Similarly, the preparation of *N,N'*-bis[(benzyloxy)carbonyl]-L-cystine by supramolecular catalysis of the coupling between two *N*-[(benzyloxy)carbonyl]-L-cysteines, that are held in favorable proximity to each other by binding to the two CONH(py) groups of the helicopodand, will be explored with optically active receptor [29].

## Experimental Part

*General.* Reagent-grade chemicals were purchased from *Aldrich* or *Fluka* and used without further purification. Compound **7** was prepared according to [30]. THF was freshly distilled from Na under N<sub>2</sub>. HPLC: *Knauer* HPLC pump 64; *t<sub>R</sub>* in min. LC: *Merck* silica gel 60 (0.040–0.063 mm, 230–400 mesh). TLC: *Merck* silica gel 60 *F*<sub>254</sub> anal. plates. M.p.: *Büchi-510* apparatus; uncorrected. UV/VIS ( $\lambda_{\text{max}}$  [nm] ( $\epsilon$ )): *Varian Cary 5*. IR ( $\tilde{\nu}$  [cm<sup>-1</sup>]): *Perkin-Elmer FTIR 1600*. <sup>1</sup>H- and <sup>13</sup>C-NMR Spectra: *Bruker AM 360* and *AMX 500* and *Varian Gemini 200*;  $\delta$ (H) [ppm] in CDCl<sub>3</sub> rel. to internal Me<sub>4</sub>Si, in (CD<sub>3</sub>)<sub>2</sub>SO rel. to the solvent peak (*quint.* at 2.49);  $\delta$ (C) [ppm] rel. to solvent peaks (CDCl<sub>3</sub>, *t* at 77.00; (CD<sub>3</sub>)<sub>2</sub>SO, *sept.* at 39.50). MS (*m/z*, %): *VG Analytical Tribrid*. Elemental analyses: Mikrolabor des Laboratoriums für Organische Chemie at ETHZ.

*Computational Studies.* MacroModel v.3.5 and BatchMin v.3.5 running on a *Silicon Graphics Crimson* work station were used for all computations, and the GB/SA solvation model [28] for CHCl<sub>3</sub> was applied in all simulations of complexes. AMBER\* and OPLS\* force fields were unmodified, but pyridine parameters were added to MM3\* (Table 4).

Table 4. Pyridine Parameters as Used in MM3\*.  
The force constants were modified to be similar to MM3\*'s benzene force constants.

C	Gen pyridinoid from AMBER*					
9	N2*CU*C2*C2*C2*C2*1					
-2						
1	1	2		1.3270	10.0000	-1.5616
2	2	1	6	115.0000	0.8000	
2	1	2	3	125.0000	0.8000	
4	00	1	2	00	0.0000	0.8000
-3						
S	Pyridine (G86 charges + dipoles + quadrupoles)					
9	N2*C2*C2*C2*C2*C2*1					
-2	<i>Force constant</i>					
1	1	2		1.3270	10.0000	
1	1	6		1.3270	10.0000	
1	2	3		1.3850	10.0000	
1	5	6		1.3850	10.0000	
2	2	1	6	115.0000	0.5000	
2	1	2	3	125.0000	0.8000	
2	5	6	1	125.0000	0.8000	
7	1	H2		75.5700	0.8500	
7	1	H3		75.5700	0.8500	
7	1	H4		75.5700	0.8500	
10	1	2	6	0.0000	0.0000	-0.9407
10	1	2	6	0.0000	0.0000	0.0000
10	1	2	6	-0.3758	0.0435	
-4						
8	-0.4900	0.2300	-0.0300	0.0900	-0.0300	0.2300
A1	Monopole charges					
11	-0.1400	-0.0400	-0.0700	0.0800	-0.0700	-0.0400

Starting structures for MC searches were generated through graphic input. Only structures which were less than 25 kJ/mol from the current lowest-energy structure were stored. At each MC step, the starting geometry was taken from among the least used stored conformations. The sets of output structures from the MC searches were minimized to 0.01 kJ/mol Å<sup>-1</sup> using the *Polak-Ribière* conjugate gradient method.

*X-Ray Crystal Structures of* (±)-Diethyl [7]*Helicene-2,17-dicarboxylate* (= (±)-Diethyl Dinaphtho[2,1-*c:1',2'-g*]phenanthrene-2,17-dicarboxylate; **3**) and (±)-N,N'-Bis(6-methylpyridin-2-yl)[7]*Helicene-2,17-dicarboxamide* (= (±)-N,N'-Bis(6-methylpyridin-2-yl)dinaphtho[2,1-*c:1',2'-g*]phenanthrene-2,17-dicarboxamide; **2**). Diester **3** (C<sub>36</sub>H<sub>26</sub>O<sub>4</sub>, *M<sub>r</sub>* 522.6) crystallized in the triclinic space group *P* $\bar{1}$  with *a* = 7.793(3), *b* = 12.764(4),

$c = 14.872(4)$  Å,  $\alpha = 111.496(7)$ ,  $\beta = 102.180(7)$ ,  $\gamma = 93.431(9)^\circ$ ,  $V = 1330$  Å<sup>3</sup>, and  $Z = 2$ . Dicarboxamide **2** ( $C_{44}H_{30}N_4O_2$ ,  $M_r$  646.8) crystallized in the monoclinic space group  $P2_1/a$  with  $a = 14.746(2)$ ,  $b = 16.240(2)$ ,  $c = 31.583(4)$  Å,  $\beta = 99.343^\circ$ ,  $V = 7463$  Å<sup>3</sup>, and  $Z = 8$ . Data were collected on a *Huber* diffractometer (**3**) constructed by Prof. C.E. Strouse and on a *Syntex-P1* diffractometer (**2**) modified by Prof. C.E. Strouse of the Department of Chemistry and Biochemistry of UCLA, using  $MoK_\alpha$  (**3**) and  $CuK_\alpha$  (**2**) radiation, to a maximum  $2\theta = 45^\circ$  (**3**) and  $100^\circ$  (**2**), giving 4168 (**3**) and 7681 (**2**) unique reflections, respectively. The structures were solved by statistical methods (SHELX86). The final discrepancy index was  $R = 0.079$  (**3**) and  $0.123$  (**2**),  $R_w = 0.067$  (**3**) and  $0.118$  (**2**) for 2949 (**3**) and 3602 (**2**) independent reflections with  $I > \sigma(I)$  (**3**) and  $I > 2\sigma(I)$  (**2**). Collection and data reduction: A yellow crystal of **3** was mounted on the *Huber* diffractometer and a yellow crystal of **2** on a fiber on the *Syntex-P1* diffractometer. Unit-cell parameters were determined from a least-squares fit of 16 (**3**) and 26 (**2**) accurately centered reflections ( $11.6^\circ < 2\theta < 20.3^\circ$  (**3**) and  $16.7^\circ < 2\theta < 35.6^\circ$  (**2**)). Data were collected at  $25^\circ$  in the  $\theta$ - $2\theta$  scan mode. Three intense reflections (1 3 1, 0 2 -7, 2 2 -4 for **3** and 0 0 7, 4 0 2, 2 3 2 for **2**) were monitored every 97 reflections to check stability. Intensities of these reflections did not decay and fluctuated a maximum of  $\pm 3.2\%$  for **3** but decayed to 15% for **2** during the course of the experiment (78.4 h (**3**) and 157.9 h (**2**)). Of the 4168 (**3**) and 7681 (**2**) unique reflections measured, 2949 (**3**) and 3602 (**2**) were considered observed ( $I > \sigma(I)$  (**3**) and  $I > 2\sigma(I)$  (**2**)) and were used in the subsequent structure analysis. Data were corrected for *Lorentz* and polarization effects (**3** and **2**), but not for secondary extinction, decay, or absorption in the case of **3**; correction was achieved also for secondary extinction and decay, but not for absorption in the case of **2**. Programs used in this work include locally modified versions of the following programs: CARESS (*Broach, Coppens, Becker, and Blessing*), peak-profile analysis, *Lorentz* and polarization corrections; SHELX86 (*Sheldrick*) structure-solution package, SHELX76 (*Sheldrick*) crystal-structure package, and ORTEP (*Johnson*). Solution and refinement (for **3**, 367 parameters were refined): Atoms were located by use of direct methods (SHELX86). All calculations were performed on a *VAX 3100* computer in the *J.D. McCullough* X-ray Crystallography Laboratory (UCLA). For **3**, all non-H-atoms were refined isotropically, and all H-atoms were included in calculated positions, C–H = 1.0 Å, with assigned isotropic thermal parameters based on those of the attached non-H-atoms. For **2**, 3 Cl-atoms of one of the 2  $CHCl_3$  molecules were refined anisotropically, the other  $CHCl_3$  molecule is disordered; two sets of Cl positions with occupancies of 0.7 and 0.3 were included for this molecule; occupancies were not refined. All other non-H-atoms of **2** were refined isotropically. H-atoms on N and on the ordered  $CHCl_3$  were included in located positions. All other H-atoms were included in calculated positions, C–H = 1.0 Å, with assigned isotropic thermal parameters based on those of the attached non-H-atoms. Scattering factors were taken from [31]. The larger peaks on a final difference electron density map were  $0.1 \text{ e } \text{\AA}^{-3}$  for **3** and  $0.4 \text{ e } \text{\AA}^{-3}$  for **2** (situated near the disordered  $CHCl_3$ ). Final positional and thermal parameters for all atoms, bond lengths, bond angles, and listing of observed and calculated structure factors were deposited for both **2** and **3** with the *Cambridge Crystallographic Data Centre*, 12 Union Road, Cambridge CB2 1EZ, England.

<sup>1</sup>H-NMR Complexation Studies. For the preparation of samples, see [32]. During the binding titrations, the guest concentration was varied (Table 5) and the changes in chemical shift of protons of **2**, held at constant

Table 5. Selected Examples of <sup>1</sup>H-NMR Binding Titration Data at 300 K in  $CDCl_3$

Run	Concentration <sup>a)</sup> [mM]	Proton of <b>2</b> <sup>b)</sup>	$\Delta\delta(\text{obs})^c)$	$\Delta\delta(\text{sat})^d)$	% sat. <sup>e)</sup>
1	[ <b>2</b> ] = 0.98, [ <b>10</b> ] = 5.00	NH	0.465	0.933	50
2	[ <b>2</b> ] = 0.83, [ <b>11</b> ] = 5.00	H–C(6)	0.166	0.239	70
		H–C(5')	0.117	0.168	70
		NH	1.502	2.048	73
3	[ <b>2</b> ] = 0.86, [ <b>12</b> ] = 6.00	H–C(6)	0.227	0.256	89
		NH	1.830	2.038	90
4	[ <b>2</b> ] = 1.03, [ <b>13</b> ] = 3.50	H–C(5')	0.182	0.209	90
		NH	1.861	2.071	87

<sup>a)</sup> Highest guest concentration at which  $\Delta\delta(\text{obs})$  was determined.

<sup>b)</sup> The arbitrary numbering shown in Fig. 7 is used.

<sup>c)</sup> Maximum observed complexation-induced change in <sup>1</sup>H-NMR chemical shift.

<sup>d)</sup> Complexation-induced change in <sup>1</sup>H-NMR chemical shift calculated for saturation binding.

<sup>e)</sup> Percent of saturation binding observed during the titration.

concentration, were monitored and evaluated. The association constants  $K_a$  and binding free energies  $-\Delta G^0$  were calculated from the titration curves by a nonlinear least-squares treatment using the program ASSOCIATE v.1.4.1. Blake Peterson, ETH-Zürich. Table 5 shows the maximum observed complexation-induced changes in chemical shifts of host protons  $\Delta\delta(\text{obs})$  and the calculate changes at saturation binding  $\Delta\delta(\text{sat})$ . All  $K_a$  and  $-\Delta G^0$  values result from duplicate or triplicate runs.

**2-Methylpropyl 4-Formylbenzoate (5).** A mixture of **4** (4.10 g, 25 mmol) and a small amount of TsOH was heated to reflux in *i*-BuOH (75 ml) for 3 d (bath temp. 180°). Besides some starting material ( $R_f$  0.26), TLC ( $\text{SiO}_2$ ,  $\text{CH}_2\text{Cl}_2$ ) indicated formation of **5** ( $R_f$  0.38) and **6** ( $R_f$  0.46). After cooling to r.t., the mixture was washed with  $\text{H}_2\text{O}$  (3  $\times$ ) and the solvent evaporated. The crude product was dissolved in 1,4-dioxane (50 ml) and 0.12N HCl (25 ml) added dropwise until two phases appeared. The mixture was stirred at r.t. and the hydrolysis of **6** monitored by TLC. After 3 h, the mixture was extracted with hexane, the combined extract washed with  $\text{H}_2\text{O}$ , sat. aq.  $\text{NaHCO}_3$  soln., and  $\text{H}_2\text{O}$  again, dried ( $\text{MgSO}_4$ ), and evaporated: pale yellow oil which was purified by fractionated distillation at 0.02 Torr: 3 g (58%) of **5**. B.p. 73–75°/0.02 Torr. The colorless oil crystallized in the freezer at  $-20^\circ$  and should be stored under  $\text{N}_2$  to prevent oxidation. IR (KBr): 3060w, 2964s, 2875m, 2839m, 2732w, 1715s, 1610w, 1578m, 1503m, 1470s, 1418m, 1378s, 1273s, 1201s, 1105s, 1016s, 981s, 947w, 855m, 836m, 800s, 759s, 689m, 514w, 468w.  $^1\text{H-NMR}$  (200 MHz,  $\text{CDCl}_3$ ): 0.99 (*d*,  $J = 6.7$ , 6 H); 2.06 (*sept.*,  $J = 6.7$ , 1 H); 4.09 (*d*,  $J = 6.7$ , 2 H); 7.90 (*d*,  $J = 8.2$ , 2 H); 8.15 (*d*,  $J = 8.2$ , 2 H); 10.05 (*s*, 1 H).  $^{13}\text{C-NMR}$  (50.3 MHz,  $\text{CDCl}_3$ ): 19.04; 27.75; 71.43; 129.37; 129.98; 135.32; 138.98; 165.39; 191.49. Anal. calc. for  $\text{C}_{12}\text{H}_{14}\text{O}_3$  (206.2): C 69.89, H 6.84; found: C 69.82, H 6.86.

**Bis(2-methylpropyl)-4,4'-[(Phenanthrene-3,6-diyl)bis(ethene-1,2-diyl)]bis(benzoate) (8).** To a suspension of **7** (3.8 g, 4.3 mmol) and **5** (1.84 g, 8.9 mmol) in dry THF (20 ml) was added dropwise a soln. of Na(*i*-BuO) prepared by dissolving Na (0.3 g, 13.4 mmol) in *i*-BuOH (20 ml). After stirring for 2 d at r.t., the mixture was cooled with an ice bath and quenched by addition of  $\text{H}_2\text{O}$ .  $\text{Et}_2\text{O}$  was added until phase separation occurred. The aq. phase was extracted once more with THF/ $\text{Et}_2\text{O}$  and the combined org. extract washed with  $\text{H}_2\text{O}$  until neutral, dried ( $\text{MgSO}_4$ ), and evaporated. LC ( $\text{SiO}_2$ ,  $\text{CH}_2\text{Cl}_2$ /hexane 3:1,  $R_f$  0.21) yielded 2.0 g (80%) of **8** as a greenish yellow honey-like paste containing three isomers (HPLC, *Vydac 201TP54*, *RP C18*,  $250 \times 4.6$  mm, MeCN/toluene 9:1, 1.0 ml/min, detection at 310 nm;  $t_R$  3.60, 5.03, 6.05), which was used without further purification in the next conversion. EI-MS: 582.3 (100,  $M^+$ ), 526.3 (7,  $[M - \text{C}_4\text{H}_8]^+$ ), 509.3 (4,  $[M - \text{C}_4\text{H}_9\text{O}]^+$ ), 453.2 (5,  $[M - \text{C}_4\text{H}_8 - \text{C}_4\text{H}_9\text{O}]^+$ ), 424.2 (2,  $[M - \text{CO}_2\text{C}_4\text{H}_9 - \text{C}_4\text{H}_9]^+$ ), 380.2 (3,  $[M - 2 \text{CO}_2\text{C}_4\text{H}_9]^+$ ).

**( $\pm$ )-Bis(2-methylpropyl) [7]Helicene-2,17-dicarboxylate ( $(\pm)$ -Bis(2-methylpropyl) Dinaphtho[2,1-*c*:1',2'-*g*]phenanthrene-2,17-dicarboxylate 9).** In a photoreactor equipped with a  $\text{H}_2\text{O}$ -cooled immersion well, a 450-W high-pressure Hg lamp and a gas inlet, a soln. of **8** (500 mg, 0.86 mmol),  $\text{I}_2$  (457 mg, 1.8 mmol), and methyloxirane (13.5 ml, 180 mmol) in toluene (1.5 l) was irradiated for 18 h under  $\text{N}_2$ . After evaporation, the crude product was washed with pentane and chromatographed ( $\text{SiO}_2$ , toluene): 260 mg (52%) of **9** ( $R_f$  0.08). M.p. 222°. IR (KBr): 3047w, 2960m, 2872w, 1705s, 1618w, 1469w, 1291s, 1248s, 1123s, 1102m, 997m, 849s.  $^1\text{H-NMR}$  (500 MHz,  $\text{CDCl}_3$ ): 0.88 (*d*,  $J = 6.7$ , 6 H); 0.93 (*d*,  $J = 6.7$ , 6 H); 1.94 (*sept.*,  $J = 6.7$ , 2 H); 3.85 (*dd*,  $J = 10.5$ , 6.5, 2 H); 3.99 (*dd*,  $J = 10.5$ , 6.5, 2 H); 7.30 (*d*,  $J = 8.3$ , 2 H); 7.41 (*d*,  $J = 8.4$ , 2 H); 7.51 (*dd*,  $J = 8.3$ , 1.6, 2 H); 7.71 (*d*,  $J = 8.6$ , 2 H); 7.90 (*d*,  $J = 8.3$ , 2 H); 7.99 (*d*,  $J = 1.6$ , 2 H); 8.01 (*d*,  $J = 8.2$ , 2 H); 8.03 (*s*, 2 H).  $^{13}\text{C-NMR}$  (125.8 MHz,  $\text{CDCl}_3$ ): 19.26; 19.31; 27.78; 70.56; 124.69; 124.88; 125.40; 126.28; 126.42; 126.77; 127.21; 127.45; 127.49; 127.86; 128.27; 128.47; 131.52; 132.32; 134.04; 166.18. EI-MS: 578.2 (100,  $M^+$ ), 505.2 (2,  $[M - \text{C}_4\text{H}_9\text{O}]^+$ ), 466.1 (3,  $[M - 2 \text{C}_4\text{H}_8]^+$ ), 421.1 (2,  $[M - \text{CO}_2\text{C}_4\text{H}_9 - \text{C}_4\text{H}_8]^+$ ), 374.1 (15,  $[M - 2 \text{CO}_2\text{C}_4\text{H}_9 - 2 \text{H}]^+$ ). Anal. calc. for  $\text{C}_{40}\text{H}_{34}\text{O}_4$  (578.71): C 83.02, H 5.92; found: C 82.81, H 6.04.

**Diethyl Ester 3.** It was prepared in a very similar way to **9** (**7**  $\rightarrow$  **8**  $\rightarrow$  **9**). M.p. 246–247°. IR (KBr): 3050w, 3039w, 2976w, 2952w, 2933w, 1710s, 1616w, 1462w, 1365w, 1294m, 1252m, 1118m, 1102m, 1018w, 848m, 756w, 602w, 528m.  $^1\text{H-NMR}$  (360 MHz,  $\text{CDCl}_3$ ): 1.31 (*t*,  $J = 7.2$ , 6 H); 4.1–4.25 (*m*, 4 H); 7.32 (*d*,  $J = 8.3$ , 2 H); 7.45 (*d*,  $J = 8.5$ , 2 H); 7.52 (*dd*,  $J = 8.3$ , 1.7, 2 H); 7.74 (*d*,  $J = 8.6$ , 2 H); 7.93 (*d*,  $J = 8.3$ , 2 H); 8.00 (*d*,  $J = 1.0$ , 2 H); 8.07 (*d*,  $J = 8.3$ , 2 H); 8.07 (*s*, 2 H).  $^{13}\text{C-NMR}$  (90.6 MHz,  $\text{CDCl}_3$ ): 14.31; 60.39; 125.76; 124.95; 125.30; 126.39; 126.43; 126.82; 127.25; 127.45; 127.50; 127.92; 128.27; 128.37; 131.53; 132.37; 134.06; 166.21.

**Dicarboxamide 2.** BuLi (2M in hexane; 0.7 ml, 1.4 mmol) was added at r.t. to a soln. of 6-methylpyridin-2-amine (162 mg, 1.5 mmol) in dry THF (8 ml). After stirring for 15 min, **9** (130 mg, 0.22 mmol) in dry THF (3 ml) was added dropwise. After stirring the mixture for 2 d, the reaction was quenched with  $\text{H}_2\text{O}$  and  $\text{Et}_2\text{O}$  added until phase separation occurred. The aq. phase was extracted with THF/ $\text{Et}_2\text{O}$ , the combined org. extracts washed with  $\text{H}_2\text{O}$  until neutral, dried ( $\text{MgSO}_4$ ), and evaporated. LC ( $\text{SiO}_2$ ,  $\text{CHCl}_3$ ,  $R_f$  0.06) yielded 134 mg (93%) of **2**. M.p. 299–300°. UV/VIS ( $\text{CHCl}_3$ ): 249 (55300), 287 (61400), 333 (sh, 14000), 365 (sh, 6900). IR (KBr): 3381m, 3054w, 2958w, 2022w, 1671s, 1662s, 1598m, 1577m, 1525s, 1453s, 1391m, 1233m, 849s, 790m.  $^1\text{H-NMR}$  (360 MHz,  $\text{CDCl}_3$ ): 6.98 (*d*,  $J = 7.6$ , 2 H); 7.45 (*d*,  $J = 8.4$ , 2 H); 7.55 (*dd*,  $J = 8.4$ , 2 H); 7.56 (*dd*,  $J = 8.1$ , 1.8, 2 H); 7.63 (*s*, 2 H); 7.63 (*dd*,  $J = 7.9$ , 7.7, 2 H); 7.78 (*s*, 2 H); 7.89 (*d*,  $J = 8.5$ , 2 H); 8.03 (*d*,  $J = 8.0$ , 2 H); 8.12 (*d*,  $J = 8.1$ , 2 H); 8.14 (*s*,



2 H); 8.14 (*d*, *J* = 8.1, 2 H).  $^{13}\text{C}$ -NMR (90.6 MHz,  $\text{CDCl}_3$ ): 24.20; 110.69; 119.01; 123.04; 124.22; 124.35; 126.89; 127.56; 127.68; 127.72; 128.06; 128.27; 128.49; 128.57; 129.63; 130.94; 132.64; 133.75; 138.46; 150.91; 156.74; 164.99. EI-MS: 646.3 (87,  $M^+$ ), 539.2 (41,  $[M - \text{C}_6\text{H}_7\text{N}_2]^+$ ), 511.3 (15,  $[M - \text{C}_7\text{H}_7\text{N}_2\text{O}]^+$ ), 430.1 (5,  $[M - 2\text{C}_6\text{H}_8\text{N}_2]^+$ ), 403.2 (8,  $[M - \text{C}_7\text{H}_7\text{N}_2\text{O} - \text{C}_6\text{H}_7\text{N}_2]^+$ ), 374.1 (72,  $[M - 2\text{C}_7\text{H}_8\text{N}_2\text{O}]^+$ ), 187.2 (100).

**Methyl 3-(cyclohexylamino)propanoate.** A mixture of methyl acrylate (1.50 g, 17.46 mmol) and cyclohexylamine (1.73 g, 17.46 mmol) in THF (5 ml) was stirred at r.t. for 2 d. The solvent was evaporated: 2.94 g (91%) of colorless oil. IR (neat): 3321 (N–H), 1738 (C=O).  $^1\text{H}$ -NMR (500 MHz,  $\text{CDCl}_3$ ): 1.26 (*m*, 5 H); 1.70 (*m*, 5 H); 2.38 (*dt*, *J* = 6.7, 3.8, 1 H); 2.47 (*t*, *J* = 6.6, 2 H); 2.85 (*t*, *J* = 6.6, 2 H); 3.63 (*s*, 3 H).  $^{13}\text{C}$ -NMR (125 MHz,  $\text{CDCl}_3$ ): 173.2; 56.5; 51.4; 41.9; 34.7; 33.4; 26.1; 24.9. EI-MS (50 eV): 185.1 ( $M^+$ ).

**4-[(2-Carboxyethyl)cyclohexylamino]-4-oxobutanoic Acid (12).** A mixture of monomethyl succinate (0.713 g, 5.4 mmol), 1*H*-benzotriazol-1-ol (0.839 g, 5.4 mmol), and *N,N*-dicyclohexylcarbodiimide (1.23 g, 5.9 mmol) in THF (20 ml) was stirred at 0° for 1 h. After addition of methyl 3-(cyclohexylamino)propanoate (1.00 g, 5.4 mmol), the mixture was stirred for 6 h and then filtered. The filtrate was evaporated, the residue dissolved in  $\text{CHCl}_3$ , and the extract washed with 1*M*  $\text{NaHCO}_3$ , 1*M*  $\text{HCl}$ , 1*M*  $\text{NaHCO}_3$ , and  $\text{H}_2\text{O}$ , dried ( $\text{MgSO}_4$ ), and evaporated. The residue was heated for 3 h in  $\text{MeOH}$  (10 ml) and 1*M*  $\text{KOH}$  (10 ml) to hydrolyze the ester. The basic soln. was washed rapidly with  $\text{AcOEt}$ , the aq. layer acidified (1*N*  $\text{HCl}$ ) and extracted with  $\text{AcOEt}$ , and the extract dried ( $\text{Na}_2\text{SO}_4$ ) and evaporated. Trituration with hexane gave 1.01 g (62%) of **12**. M.p. 183–185°. IR (KBr): 2942 (O–H), 1707, 1609 (C=O).  $^1\text{H}$ -NMR (200 MHz,  $(\text{CD}_3)_2\text{SO}$ , 353 K): 1.41 (*m*, 11 H); 2.44 (*m*, 4 H); 3.39 (*m*, 4 H);  $^{13}\text{C}$ -NMR (125 MHz,  $(\text{CD}_3)_2\text{SO}$ , 363 K): 172.9; 171.7; 170.2; 34.4; 30.3; 29.0; 27.6; 25.0; 24.8; 24.4; 23.9. Anal. calc. for  $\text{C}_{13}\text{H}_{21}\text{NO}_5$  (271.31): C 57.55, H 7.80, N 5.16; found: C 57.39, H 8.11, N 5.40.

**(E)-4-[(2-Carboxyethyl)cyclohexylamino]-4-oxobut-2-enoic Acid (13).** Starting from monoethyl fumarate, the same procedure as described for **12** was applied, except for 24 h instead of 3 h reaction time for the ester hydrolysis: 1.10 g (65%) of **13**. M.p. 186–188°. IR (KBr): 2940 (O–H), 1714, 1613 (C=O).  $^1\text{H}$ -NMR (200 MHz,  $(\text{CD}_3)_2\text{SO}$ , 353 K): 1.39 (*m*, 11 H); 2.44 (*t*, *J* = 8.1, 2 H); 3.52 (*t*, *J* = 8.1, 2 H); 6.73 (*d*, *J* = 15.6, 1 H); 7.31 (*d*, *J* = 15.6, 1 H). Anal. calc. for  $\text{C}_{13}\text{H}_{19}\text{NO}_5$  (269.30): C 57.98, H 7.11, N 5.20; found: C 57.61, H 6.95, N 5.70.

**(Z)-4-[(2-Carboxyethyl)cyclohexylamino]-4-oxobut-2-enoic Acid (11).** A mixture of maleic anhydride (400 mg, 4.08 mmol) and methyl 3-(cyclohexylamino)propanoate **17** (1.512 g, 8.16 mmol) in dry THF (5 ml) was stirred for 15 h. The solvent was removed and the residue stirred for 3 h in  $\text{MeOH}$  (10 ml) and 1*M*  $\text{KOH}$  (10 ml). Workup as described for **12** gave 746 mg (68%) of **11**. M.p. 173–175°. IR ( $\text{CHCl}_3$ ): 3015 (O–H), 1713, 1621, 1559 (C=O),  $^1\text{H}$ -NMR (200 MHz,  $(\text{CD}_3)_2\text{SO}$ , 353 K): 1.40 (*m*, 11 H); 2.42 (*t*, *J* = 4.0, 2 H); 3.38 (*t*, *J* = 4.0, 2 H); 5.91 (*dt*, *J* = 12.0, 1 H); 6.73 (*d*, *J* = 12.0, 1 H).  $^{13}\text{C}$ -NMR (125 MHz,  $(\text{CD}_3)_2\text{SO}$ , 363 K): 172.4; 165.8; 165.1; 136.5; 123.8; 30.2; 24.9; 24.3; 23.6; 23.3; 21.2. Anal. calc. for  $\text{C}_{13}\text{H}_{19}\text{NO}_5$  (269.30): C 57.98, H 7.11, N 5.20; found: C 57.45; H 7.17; N 5.75.

The initial part of this work at UCLA was supported by the *National Institutes of Health* and a postdoctoral fellowship to C.T. from *NATO* and the Grand-Duchy of Luxembourg.

## REFERENCES

- [1] D. J. Cram, J. M. Cram, *Acc. Chem. Res.* **1978**, *11*, 8; D. J. Cram, K. N. Trueblood, *Top. Curr. Chem.* **1981**, *98*, 43; C. B. Knobler, F. C. A. Gaeta, D. J. Cram, *J. Chem. Soc., Chem. Commun.* **1988**, 330.
- [2] V. Prelog, *Pure Appl. Chem.* **1978**, *50*, 893; b) V. Prelog, S. Mutak, *Helv. Chim. Acta* **1983**, *66*, 2274; c) M. Dobler, M. Dumić, M. Egli, V. Prelog, *Angew. Chem.* **1985**, *97*, 793; *ibid. Int. Ed.* **1985**, *24*, 792.
- [3] K.-S. Jeong, A. V. Muehldorf, J. Rebek, Jr., *J. Am. Chem. Soc.* **1990**, *112*, 6144.
- [4] a) P. P. Castro, T. M. Georgiadis, F. Diederich, *J. Org. Chem.* **1989**, *54*, 5835; b) V. Alcazar, F. Diederich, *Angew. Chem.* **1992**, *104*, 1503; *ibid. Int. Ed.* **1992**, *31*, 1521.
- [5] F. Garcia-Tellado, J. Albert, A. D. Hamilton, *J. Chem. Soc., Chem. Commun.* **1991**, 1761.
- [6] A. Galan, D. Andreu, A. M. Echavarren, P. Prados, J. de Mendoza, *J. Am. Chem. Soc.* **1992**, *114*, 1511; Y. Li, L. Echegoyen, M. V. Martinez-Diaz, J. de Mendoza, T. Torres, *J. Org. Chem.* **1991**, *56*, 4193.
- [7] R. Liu, P. E. J. Sanderson, W. C. Still, *J. Org. Chem.* **1990**, *55*, 5184; S. D. Erickson, J. A. Simon, W. C. Still, *ibid.* **1993**, *58*, 1305; J.-I. Hong, S. K. Namgoong, A. Bernardi, W. C. Still, *J. Am. Chem. Soc.* **1991**, *113*, 5111; W. C. Still, J. D. Kilburn, P. E. J. Sanderson, R. P. Liu, M. R. Wiley, F. P. Hollinger, R. C. Hawley, M. Nakajima, A. Bernardi, J. I. Hong, S. K. Namgoong, *Isr. J. Chem.* **1992**, *32*, 41.
- [8] W. H. Pirkle, J. A. Burke, K. C. Deming, *J. Liq. Chromatogr.* **1993**, *16*, 161; W. H. Pirkle, T. C. Pochapsky, *Chem. Rev.* **1989**, *89*, 347; W. H. Pirkle, C. J. Welch, B. Lamm, *J. Org. Chem.* **1992**, *57*, 3854.
- [9] W. H. Laarhoven, W. J. C. Prinsen, *Top. Curr. Chem.* **1984**, *125*, 63; K. P. Meurer, F. Vögtle, *ibid.* **1985**, *127*, 1; R. H. Martin, *Angew. Chem.* **1974**, *86*, 727; *ibid. Int. Ed.* **1974**, *13*, 649.

- [10] a) L. Liu, B. Yang, T. J. Katz, M. K. Poindexter, *J. Org. Chem.* **1991**, *56*, 3769; b) T. J. Katz, A. Sudhakar, M. F. Teasley, A. M. Gilbert, W. E. Geiger, M. P. Robben, M. Wuensch, M. D. Ward, *J. Am. Chem. Soc.* **1993**, *115*, 3182; c) C. A. Liberko, L. L. Miller, T. J. Katz, L. Liu, *ibid.* **1993**, *115*, 2478; d) A. M. Gilbert, T. J. Katz, W. E. Geiger, M. P. Robben, A. L. Rheingold, *ibid.* **1993**, *115*, 3199; e) N. D. Willmore, L. Liu, T. J. Katz, *Angew. Chem.* **1992**, *104*, 1081, *ibid. Int. Ed.* **1992**, *31*, 1093.
- [11] K. Deshayes, R. D. Broene, I. Chao, C. D. Knobler, F. Diederich, *J. Org. Chem.* **1991**, *56*, 6787.
- [12] F. Vögtle, E. Weber, *Angew. Chem.* **1979**, *91*, 837; *ibid. Int. Ed.* **1979**, *18*, 753.
- [13] C. Vincent, E. Fan, A. D. Hamilton, *Tetrahedron Lett.* **1992**, *33*, 4269; F. Garcia-Tellado, S. Goswami, S.-K. Chang, S. J. Geib, A. D. Hamilton, *J. Am. Chem. Soc.* **1990**, *112*, 7393; R. P. Dixon, S. J. Geib, A. D. Hamilton, *ibid.* **1992**, *114*, 365; V. Jubian, R. P. Dixon, A. D. Hamilton, *ibid.* **1992**, *114*, 1120; E. Fan, S. A. Van Arman, S. Kincaid, A. D. Hamilton, *ibid.* **1993**, *115*, 369.
- [14] a) V. Alcazar, L. Tomlinson, K. N. Houk, F. Diederich, *Tetrahedron Lett.* **1991**, *32*, 5309; b) V. Alcazar, J. R. Moran, F. Diederich, *Isr. J. Chem.* **1992**, *32*, 69.
- [15] F. B. Mallory, C. Mallory, *Org. React.* **1984**, *30*, 1.
- [16] T. W. Bell, H. Jouselin, *J. Am. Chem. Soc.* **1991**, *113*, 6283; K. Yamamoto, T. Ikeda, T. Kitsuki, Y. Okamoto, H. Chikamatsu, M. Nakazaki, *J. Chem. Soc., Perkin Trans. 1*, **1990**, 271.
- [17] C.-Y. Huang, V. Lynch, E. V. Anslyn, *Angew. Chem.* **1992**, *104*, 1259; *ibid. Int. Ed.* **1992**, *31*, 1244; S. J. Geib, C. Vicent, E. Fan, A. D. Hamilton, *ibid.* **1993**, *105*, 83 and **1993**, *32*, 119; J. Yang, E. Fan, S. J. Geib, A. D. Hamilton, *J. Am. Chem. Soc.* **1993**, *115*, 5314; M. Mascal, C. J. Moody, A. I. Morrell, A. M. Z. Slawin, D. J. Williams, *ibid.* **1993**, *115*, 813.
- [18] a) P. T. Beurskens, G. Buerskens, Th. E. M. van den Hark, *Acta Crystallogr., Sect. C, Cryst. Struct. Commun.* **1976**, *5*, 241; b) Th. E. M. van den Hark, P. T. Beurskens, *Acta Crystallogr., Sect. C, Cryst. Struct. Commun.* **1976**, *5*, 247; c) W. Marsh, J. D. Dunitz, *Bull. Soc. Chim. Belg.* **1979**, *88*, 847; d) M. Joly, N. Defay, R. H. Martin, J. P. Declercq, G. Germain, B. Soubrier-Payen, M. Van Meerse, *Helv. Chim. Acta* **1977**, *60*, 537; e) J. Navaza, G. Toucaris, G. Le Bas, A. Navaza, C. de Rango, *Bull. Soc. Chim. Belg.* **1979**, *88*, 863; f) J. B. M. Somers, J. H. Borkent, W. H. Laarhoven, *Recl. Trav. Chim. Pays-Bas* **1981**, *100*, 110.
- [19] R. A. Pascal, *Pure Appl. Chem.* **1993**, *65*, 105; L. T. Scott, M. M. Hashemi, M. S. Bratcher, *J. Am. Chem. Soc.* **1992**, *114*, 1920; A. Borchardt, A. Fuchicello, K. V. Kilway, K. K. Balridge, J. S. Siegel, *ibid.* **1992**, *114*, 1921; A. H. Abdourazak, A. Sygula, P. W. Rabideau, *ibid.* **1993**, *115*, 3010; M. Shen, I. S. Ignatyev, Y. Xie, H. F. Schaefer, III, *J. Phys. Chem.* **1993**, *97*, 3212; K. B. Lipkowitz, M. A. Peterson, *J. Comput. Chem.* **1993**, *14*, 121.
- [20] H. J. Lindner, *Tetrahedron* **1975**, *31*, 281; N. L. Allinger, J. T. Sprague, *J. Am. Chem. Soc.* **1973**, *95*, 3893; W. C. Herndon, P. C. Nowak, D. A. Connor, P. Lin, *ibid.* **1992**, *114*, 41; I. Chao, Ph. D. Thesis, University of California, Los Angeles, 1991.
- [21] U. Burkett, N. L. Allinger, 'Molecular Mechanics', ACS Monograph 177, American Chemical Society, Washington, D.C., 1982.
- [22] N. L. Allinger, Y. H. Yuh, J.-H. Lii, *J. Am. Chem. Soc.* **1989**, *111*, 8551.
- [23] S. J. Weiner, P. A. Kollman, D. A. Case, U. C. Singh, C. Ghio, G. Alagona, S. Profeta, Jr., P. Weiner, *J. Am. Chem. Soc.* **1984**, *106*, 765; S. J. Weiner, P. A. Kollman, D. T. Nguyen, D. A. Case, *J. Comput. Chem.* **1986**, *7*, 230; D. Q. McDonald, W. C. Still, *Tetrahedron Lett.* **1992**, *33*, 7743.
- [24] W. L. Jorgensen, J. Tirado-Rives, *J. Am. Chem. Soc.* **1988**, *110*, 1657.
- [25] W. C. Still, 'MacroModel v.3.5', Columbia University, New York; F. Mohamadi, N. G. J. Richards, W. C. Guida, R. Liskamp, M. Lipton, C. Caufield, G. Chang, T. Hendrickson, W. C. Still, *J. Comput. Chem.* **1990**, *11*, 440.
- [26] R. Breslow, R. Rajagopalan, J. Schwarz, *J. Am. Chem. Soc.* **1981**, *103*, 2905; E. Kimura, A. Sakonaka, T. Yatsunami, M. Kodama, *ibid.* **1981**, *103*, 3041; M. W. Hosseini, J.-M. Lehn, *ibid.* **1982**, *104*, 3525; J. Rebek, Jr., D. Nemeth, P. Ballester, F.-T. Lin, *ibid.* **1987**, *109*, 3474; Y. Tanaka, Y. Kato, Y. Aoyama, *ibid.* **1990**, *112*, 2807; A. Bencini, A. Bianchi, M. I. Burguete, E. Garcia-Espana, S. V. Luis, J. A. Ramirez, *ibid.* **1992**, *114*, 1919; P. Schiessl, F. P. Schmidtchen, *Tetrahedron Lett.* **1993**, *34*, 2449; S. S. Flack, J.-L. Chaumette, J. D. Kilburn, G. J. Langley, M. Webster, *J. Chem. Soc., Chem. Commun.* **1993**, 399.
- [27] W. C. Still, 'BatchMin v.3.5', Columbia University, New York.
- [28] W. C. Still, A. Tempczyk, R. C. Hawley, T. Hendrickson, *J. Am. Chem. Soc.* **1990**, *112*, 6127.
- [29] T. R. Kelly, C. Zhao, G. J. Bridger, *J. Am. Chem. Soc.* **1989**, *111*, 3744; T. R. Kelly, G. J. Bridger, C. Zhao, *ibid.* **1990**, *112*, 8024.
- [30] H. A. Staab, U. E. Meissner, B. Meissner, *Chem. Ber.* **1976**, *109*, 3875.
- [31] 'International Tables for X-Ray Crystallography', Kynach Press, Birmingham, England, 1974, Vol. IV.
- [32] S.-W. Tam-Chang, L. Jimenez, F. Diederich, *Helv. Chim. Acta* **1993**, *76*, 2616.